Proceedings of ICONE14
International Conference on Nuclear Engineering
July 17-20, Miami, Florida, USA

ICONE14-89103

STEADY STATE AND DYNAMIC ANALYSES OF SUPERCRITICAL CO_2 NATURAL CIRCULATION LOOP

Prashant Jain and Rizwan-uddin
Department of Nuclear, Plasma and Radiological Engineering
University of Illinois at Urbana-Champaign, 214 NEL, 103 S. Goodwin Ave
Urbana, IL 61801, USA

ABSTRACT

Numerical studies have been carried out to investigate supercritical flow instabilities in a CO_2 natural circulation loop. For the steady state and dynamic analyses of the loop under supercritical conditions, a single-channel, one-dimensional model is developed. In this model, equations for the conservation of mass, momentum and energy are discretized using an implicit finite difference scheme. A computer code called FIASCO (Flow Instability Analysis under SuperCritical Operating conditions) is developed in FORTRAN90 to simulate the dynamics of natural circulation loops with supercritical fluid. Results obtained for the stability boundary substantially deviate from the results reported by previous investigators, and thus contradict some of the reported findings. The disagreement in results is most likely due to the undesirable dissipative and dispersive effects produced from the large time steps used in previous studies, thereby leading to a larger stable region than those found using smaller time step. Results presented here suggest that the stability boundary of a natural circulation loop with supercritical fluid, is not confined to the *near-peak region* of the (steady state) flow-power curve. Additional and more extensive experimental data are needed to resolve the differences between results obtained here and those reported earlier. However, results obtained for the range of parameter values used in this investigation always predict the stability threshold to be in the positive slope region of the (steady state) flow-power curve. Parametric studies for different operating conditions reveal the similarity of stability characteristics under supercritical conditions with those in two-phase flows.

NOMENCLATURE

C_k	coefficient in momentum conservation equation
D_h	hydraulic diameter, m
f	friction coefficient
g	acceleration due to gravity, m/s^2
h	specific enthalpy, J/kg-K
i	grid index
m	index for the last grid point
n	time step index
p	pressure, N/m^2
q'''	volumetric heat addition rate, W/m^3
Re	Reynolds number
R_{k_1}	inlet restriction coefficient
R_{k_2}	exit restriction coefficient
t	time, s
u	velocity, m/s
z	axial distance, m
ρ	density, kg/m^3
θ	angle of flow direction with respect to horizontal plane, rad
μ	dynamic viscosity, N-s/m^2
η	$=\frac{\Delta z}{2\Delta t}$
Δz	spatial grid size, m
Δt	time step size, s

INTRODUCTION

Supercritical-Water-Cooled Reactor (SCWR) is one of the advanced nuclear reactor system selected under the Generation IV program for cost effective energy generation, and safety. SCWR concept has evolved from the Japanese supercritical light water reactor (SCLWR) with a thermal spectrum, cooled and moderated by supercritical light water. This reactor system has potential to improve fuel economy and can simplify plant design considerably. Moreover, compared with the Light Water Reactors, higher thermal efficiency and lower coolant mass flow rate *per unit core thermal power* can be achieved with SCWRs [1]. It is also rated good in safety, proliferation resistance and physical protection because of its passive safety features, to avoid accidents and reduce operator dependability [2].

SCWR design is built upon two well developed technologies: Light Water Reactors (LWRs) and supercritical fossil-fired boilers. In SCWR, operation at supercritical pressure (25.0 MPa) eliminates coolant boiling, so the coolant always remains in single-phase throughout the system; and superheated steam can be obtained without the danger of dryout in the core. However, a gradual deterioration in heat transfer may occur in the *near-critical region* (narrow region around the pseudo-critical point), but does not result in significant drop in the heat transfer coefficients associated with dryout [3]. Additionally, employment of single-loop cycle remarkably simplifies the nuclear system eliminating the need of recirculation lines, pressurizer, steam separators and dryers, as coolant directly circulates to and fro from the core to the turbine. In short, SCWR design takes advantage of the desirable feature of BWR over PWR (single loop) without the associated disadvantage (boiling). Moreover, the mass flow rate of coolant in SCWR is low (about 10 % of that in LWR), and core exit temperature is high with a large temperature increase across the core, thereby resulting in a high plant thermal efficiency of about 44% [1].

Due to supercritical operating conditions in SCWR, thermodynamic and transport properties of water change significantly as its temperature approaches the pseudocritical point, where the distinction between liquid and vapor phases disappears. The heat conduction coefficient and the heat capacity at constant pressure tend to increase dramatically, while the thermal diffusivity tends to zero [4]. Also, density and viscosity tend to decrease significantly as fluid temperature approaches the pseudocritical point. Some of these changes are similar in magnitude to those encountered during boiling with phase change. [It may be noted that there is no phase transition (i.e. no two phase) of water as its temperature crosses the pseudocritical point.]

Similar to BWRs, SCWR core will experience large changes in density across the core and for this reason may be susceptible to flow instabilities similar to those observed in BWRs (such as density-wave instabilities, and coupled thermohydraulic and neutronic instabilities). In addition, dramatic changes in other thermophysical properties may also lead to yet unexplored phenomena. Therefore, the licensing of SCWR will require demonstrable capability to predict the onset of instabilities. Consequently, it is necessary to understand the instability phenomena in SCWR and identify the variables which affect these phenomena. The ultimate goal is to generate stability maps to identify stable operating conditions for SCWR design [5,6].

Thermal hydraulic instabilities resulting in flow oscillations are highly undesirable in SCWR system, as they may give rise to nuclear instabilities (due to density-reactivity feedback) and result in failure of control mechanism or fatigue damage of reactor components [7]. That, in turn, will affect the heat removal system efficiency and may put the safety of reactor system in jeopardy. Moreover, emphasis is also placed on passive safety mechanisms by employing, for example, natural circulation cooling systems (rather than forced ones) after accidental reactor shutdown to remove core decay heat. Consequently, it is necessary to study SCWR stability under natural circulation conditions.

The natural circulation loop with supercritical flow conditions ─ that always remains in single phase ─ experiences a rather large density change across a very small temperature range near the pseudo-critical point. This may lead the system towards instabilities similar to those observed in heated channels with two-phase flows. Instabilities in loops with supercritical flow, associated with the two-phase like property variation of single phase supercritical fluid, near the pseudocritical point have not been fully explored. Hence, a study of flow stability phenomenon in a natural circulation loop with supercritical fluid is carried out in this paper, which can later be modified to analyze SCWR instabilities as well. To provide a comprehensive understanding, recent work on stability of supercritical fluid flow in a single-channel, natural-convection loop is reviewed. An analytical model of supercritical flow in an idealized single-channel, natural-convection configuration to study system stability is developed by Chatoorgoon [8]. The analyzed configuration is a constant cross-section area loop with constant boundary conditions for inlet temperature, inlet pressure and outlet pressure. The same point source and point sink configuration is also simulated using the SPORTS (Special Predictions Of Reactor Transients and Stability) [9] code, and good agreement is reported in obtaining bounding power for stable flows [8]. Chatoorgoon [8] also studied the supercritical flow stability phenomenon numerically in the same loop with distributed heat source and sink, using the SPORTS [9] code. More recently, Chatoorgoon et al. [10, 11] reported an extended numerical study by examining effect of several different parameters on supercritical flow stability including inlet temperatures, inlet and outlet channel restriction coefficients (K factors), different loop heights and heated lengths. In addition, this study also included effect of different fluids like CO_2 and H_2. Based on the numerical results obtained it is concluded that stability characteristics of supercritical CO_2 are very similar to that of supercritical H_2O. There have been very few experimental studies of natural circulation with fluids near the critical point. Recently, experimental results of a natural circulation supercritical water (SCW) loop at University of Wisconsin-Madison is reported in [12]. Also, experiments were performed at Argonne National Laboratory (ANL) in a rectangular test loop with CO_2 ─ in place of water ─ to allow operation at moderate temperature and pressure [13]. These experimental results deviate significantly from numerical predictions made in [11] and [12]. Hence, a study of flow stability phenomenon in a natural circulation loop geometry is carried out, which can later be modified and upgraded to analyze SCWR instabilities as well.

MODEL AND NUMERICAL ANALYSIS

Time-domain, nonlinear finite difference models are commonly used for thermohydrodynamic stability evaluations. These finite-difference techniques are usually very time consuming when used for stability analyses since the allowable time step size may be very small and large number of cases must be run to generate a stability map. However, with the advancement in computational resources, time domain investigation of flow stability has become a promising method compared with the other (frequency domain) standard approaches. This methodology involves solving transient mass, momentum and energy conservation equations by application of some numerical method. It is usually performed to predict the threshold value of a system parameter (for example, heat flux or power level) below (or above) which the system is stable. The basic idea is to first solve the flow governing equations for the steady state and then treat the steady state solution as the initial condition for the transient flow. At time $t = 0$, a perturbation is introduced into the flow system. This perturbation can be either a fractional change in initial condition (which is actually the steady state solution) or a small change in the flow governing parameters (like heat flux, pressure boundary value etc). Stability can also be investigated by momentarily perturbing the steady state, for example, with a delta-function variation of a boundary condition. If the disturbance grows in time and yields sustained or diverging flow oscillations, then the steady-state system is considered to be unstable. On the other hand, if the disturbance leads to decaying oscillations resulting in convergence of flow and other field variables to the steady state solution, then the corresponding steady-state solution is considered to be stable.

Steady state and dynamic analyses of SCWR require appropriate modeling of the thermodynamic and transport properties of water near its critical point. Due to high nonlinearities associated, multi-dimensional modeling of the coolant channel becomes too complex. Therefore, for this preliminary investigation, a single-channel, one-dimensional model is developed. In this model, equations for the conservation of mass, momentum and energy are discretized using an implicit finite difference scheme. Thermophysical properties of the supercritical fluid are determined using the NIST REFPROP 7.0 package [14]. Details of the model developed are described below.

Governing equations

For one-dimensional channel flow, the unsteady mass, momentum and energy conservation equations, and the equation of state can be written as follows:

Continuity:

$$\frac{\partial \rho}{\partial t} + \frac{\partial (\rho u)}{\partial z} = 0 \tag{1}$$

Momentum conservation:

$$\frac{\partial (\rho u)}{\partial t} + \frac{\partial (\rho u^2)}{\partial z} + \frac{\partial p}{\partial z} + C_k \rho u^2 + \rho g \sin\theta = 0 \tag{2}$$

Energy conservation:

$$\frac{\partial}{\partial t}\left[\rho\left(h + \frac{u^2}{2}\right)\right] + \frac{\partial}{\partial z}\left[\rho u\left(h + \frac{u^2}{2}\right)\right] + \rho u g \sin\theta = \frac{\partial p}{\partial t} + q''' \tag{3}$$

State:

$$\rho = eos(p, h) \tag{4}$$

where ρ, u, p and h are the fluid density, velocity, pressure and enthalpy, respectively. Also, g is the acceleration due to gravity, θ is the angle (anti-clockwise) of the flow direction from the horizontal plane, and q''' is the volumetric heat generation rate.

Coefficient C_k in momentum conservation equation is given by

$$C_k = \frac{f}{2D_h} \tag{5}$$

where D_h is the hydraulic diameter of the channel and f is the friction factor, which can be obtained from the Blasius and McAdams relations [15] for a smooth tube as:

$$f = \begin{cases} 0.316\,\mathrm{Re}^{-0.25}, & \mathrm{Re} < 30{,}000 \\ 0.184\,\mathrm{Re}^{-0.20}, & 30{,}000 < \mathrm{Re} < 10^6 \end{cases} \tag{6}$$

where Re is the Reynolds number defined as

$$\mathrm{Re} = \frac{\rho u D_h}{\mu} \tag{7}$$

and μ is the dynamic viscosity of the fluid in the channel.

The set of mass, momentum and energy conservation equations is closed by the equation of state for the supercritical fluid in the channel.

Spatial and temporal discretization

The governing equations, which form a system of non-linear equations, are solved numerically. Control-volume formulation technique in space and forward-difference scheme in time, are employed to derive finite difference equations for the mass, momentum and energy conservation.

The one-dimensional flow channel is divided into axial computational cells or control volumes, with the grid points located at the cell edges as shown in Figure 1. The first and last grid points of the domain coincide with the flow channel physical boundaries. By integrating the conservation equations for mass, momentum and energy from grid point (i) to $(i+1)$ and using forward difference approximation for the time derivative, the following set of implicit discretized equations can be written:

Continuity:

$$u_{i+1}^{n+1} = \frac{(\rho u)_i^{n+1} - \eta\left(\rho_i^{n+1} - \rho_i^n + \rho_{i+1}^{n+1} - \rho_{i+1}^n\right)}{\rho_{i+1}^{n+1}} \tag{8}$$

Momentum conservation:

$$p_{i+1}^{n+1} = p_i^{n+1} - \left(1 + \frac{1}{2}(C_k)_{i+1}^n \Delta z\right)(\rho u^2)_{i+1}^n + \left(1 - \frac{1}{2}(C_k)_i^n \Delta z\right)(\rho u^2)_i^n - \left(\frac{\rho_i^n + \rho_{i+1}^n}{2}\right) g \Delta z \sin\theta_i + \eta\left((\rho u)_i^{n+1} - (\rho u)_i^n + (\rho u)_{i+1}^{n+1} - (\rho u)_{i+1}^n\right) \tag{9}$$

Energy conservation:

$$h_{i+1}^{n+1} = \frac{\left[\left(\frac{q_i''' + q_{i+1}'''}{2}\right)\Delta z - \left(\frac{(\rho u)_{i+1}^{n+1} + (\rho u)_i^{n+1}}{2}\right) g \Delta z \sin\theta_i - \eta\left\{(\rho h)_i^{n+1} - (\rho h)_{i+1}^n - (\rho h)_i^n\right\} + (\rho u h)_i^{n+1}\right]}{(\rho u)_{i+1}^{n+1} + \eta \rho_{i+1}^{n+1}} \tag{10}$$

State:

$$\rho_{i+1}^{n+1} = function\left(p_{i+1}^{n+1}, h_{i+1}^{n+1}\right) \tag{11}$$

where the friction coefficient $(C_k)_i^n$ in equation (9) is defined by

$$(C_k)_i^n = \frac{f_i^n}{2D_h} = \frac{1}{2D_h}\begin{cases} 0.316(\mathrm{Re}^{-0.25})_i^n, & \mathrm{Re}_i^n < 30{,}000 \\ 0.184(\mathrm{Re}^{-0.20})_i^n, & 30{,}000 < \mathrm{Re}_i^n < 10^6 \end{cases} \tag{12}$$

and Re_i^n is given by

$$\mathrm{Re}_i^n = \frac{(\rho u)_i^n}{\mu_i^n} D_h \tag{13}$$

In the above set of discrete equations, η is given by $\frac{\Delta z}{2\Delta t}$ where Δz and Δt correspond to the spatial grid size and time step, respectively.

In deriving the finite difference equations, the effect of integrating across a computational cell is analogous to averaging the field and flow variables in that cell, and leads to better accuracy compared to the first order difference scheme of the spatial derivatives.

Boundary conditions

Solution of the system of non-linear governing equations depends upon the choice of boundary conditions. For the present investigation, constant pressure drop boundary condition along with constant inlet conditions are applied to the flow channel, i.e. inlet temperature, inlet pressure and outlet pressure are known.

For the case of zero total pressure drop (natural circulation) inside the flow channel, these boundary conditions may be physically achieved by connecting both ends of the channel to a large reservoir, in which constant inlet conditions are maintained [8, 11, 12].

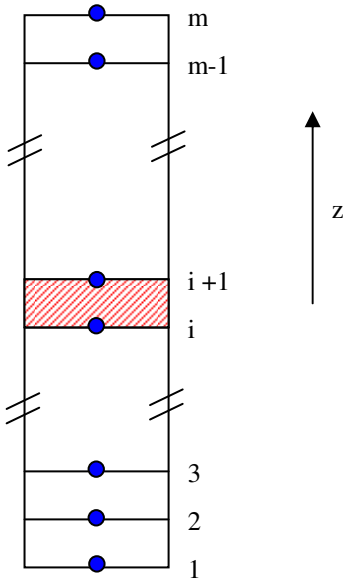

Figure 1: Spatial grid and control volume in the flow channel

Solution algorithm

Details of the solution algorithm employed to solve the coupled, nonlinear, time dependent equations, (8) to (11) are given below [9]:

I. There are four unknown variables (ρ , u , p and h) to be solved for each grid point i .

II. Initial condition: At $t = 0$, all unknown variables are assumed to be known for each grid point i .

$$\rho_i^0 = \text{known}$$
$$u_i^0 = \text{known}$$
$$p_i^0 = \text{known}$$
$$h_i^0 = \text{known}$$

III. Boundary conditions: As inlet conditions of the flow channel are maintained constant, for each $(n+1)^{th}$ time step, at grid point 1

$$\rho_1^{n+1} = \rho_{\text{in}} = \text{constant}$$
$$p_1^{n+1} = p_{\text{in}} = \text{constant}$$

$$h_1^{n+1} = h_{in} = \text{constant}$$

IV. For the $(n+1)^{th}$ time step,

a) Velocity at the channel inlet u_1^{n+1}, is guessed

b) Following steps b.1 and b.2 are repeated for i = 1,…, (m-1)

b.1) A value for ρ_{i+1}^{n+1} is guessed at the $(i+1)^{th}$ grid point.

b.2) All the variables on the RHS of the continuity equation (8) are now known. Using this equation, velocity u_{i+1}^{n+1} is calculated. This, in turn, yields solution for p_{i+1}^{n+1} and h_{i+1}^{n+1} from equations (9) and (10), respectively. Now, using this pressure and enthalpy values, state equation (11) is solved for density $\tilde{\rho}_{i+1}^{n+1}$. This step (b.2) is repeated (until a desired convergence is reached) with the updated density value $\tilde{\rho}_{i+1}^{n+1}$ serving as a guess for ρ_{i+1}^{n+1}.

c) At convergence, all the unknown variables at each grid point are calculated up to the outlet of the flow channel, where a constant exit pressure, p_{out}, is specified.

d) Calculated pressure at the outlet, p_m^{n+1}, is compared with the constant specified pressure p_{out}. If the difference $\left| p_{out} - p_m^{n+1} \right|$ is within the specified tolerance limit, then simulation moves to the next time step level. Otherwise, step IVb is repeated with another guess value (in step IVa) for u_1^{n+1} until the pressure boundary condition at the exit (grid m) is satisfied within specified tolerance. Improved guess for u_1^{n+1} can be obtained by employing either the "Bi-section method" or the "Regula-Falsi method". [Not surprisingly, Regula-Falsi lead to faster convergence than the Bi-section method.]

Numerical scheme and algorithm described above are used in the next section to simulate a supercritical CO_2 loop and study its stability characteristics.

TIME DOMAIN STABILITY ANALYSIS

A computer code called FIASCO (Flow Instability Analysis under SuperCritical Operating conditions) is developed in FORTRAN90 to simulate the dynamics of a natural circulation loop with supercritical fluid. For the validation of the code as well as to gain some insight into the natural circulation heat removal mechanism under supercritical conditions, several results available in literature [12, 13] were fist reproduced using this code.

Flow system analysis

For the time domain stability analysis and parametric studies, a simple single-channel rectangular loop (same as in [11]) is chosen. It is essentially a constant area loop with lower horizontal heating and upper horizontal cooling sections. Heat source and sink is assumed to be of equal magnitude, and uniformly distributed in the respective sections. Also, energy is assumed to be directly deposited or extracted to the respective sections eliminating the need to model wall heat transfer mechanism. Both, inlet and outlet of the loop are assumed to be connected to a large reservoir or pressurizer chamber in order to maintain constant inlet condtions (i.e. constant pressure and temperature at point A) during the operation of the loop. Also, zero total pressure drop boundary condition is applied in the flow loop, which in turn, gives another boundary condition at the outlet point, O.

The stability analysis is performed with supercritical carbon dioxide as the working fluid. [CO_2 is often used in supercritical fluid experiments due to its viability and similarity in thermo-physical properties variations compared to water at supercritical conditions.] Reservoir conditions are maintained at 25 ^oC temperature and 8 MPa pressure, which provide inlet pressure, inlet temperature and outlet pressure boundary conditions for the flow loop. Geometrical parameters for the loop are shown in the schematic diagram in Figure 2. Moreover, inlet and exit restriction loss coefficients — $R_{k_1} = 0.5$ and $R_{k_2} = 0.5$ respectively — are taken into account, by modifying C_k as,

$$C_{k_i} = \frac{f_i}{2D_h} + \frac{R_{k_i}}{\Delta z}$$ for the inlet and outlet grid points.

For given parameter values, the steady-state solution is determined first by employing the numerical approach described earlier. NIST REFPROP 7.0 package [14] is modified and linked to the FORTRAN code. It is used as the state equation to provide thermo-physical properties data for CO_2. Steady-state solution for the unknown variables (ρ, u, p and h) is used as an initial condition at every grid point for the transient simulations. It is to be noted here that perturbation can be introduced in any of the unknown variable by disturbing its steady state value fractionally. For the analysis presented here, steady state velocities are perturbed (positive) by 1 % and used as an initial condition for velocity at each grid point. Then, at

every time step, discrete variables are evaluated throughout the domain with exit pressure boundary conditions satisfying within the tolerance limit of 10^{-6} MPa. If, the perturbation grows in time, i.e. inlet velocity (and velocity at all grid points) oscillations diverge as time increases, then the system is considered to be unstable. Otherwise, if the perturbation decays in time, i.e. inlet velocity oscillations dampen and inlet velocity returns to its steady state value, then the system is considered to be stable. Power level at which flow oscillations nearly sustain their amplitude (i.e. neither diverge nor converge), is called the threshold power (stability boundary) for that flow system.

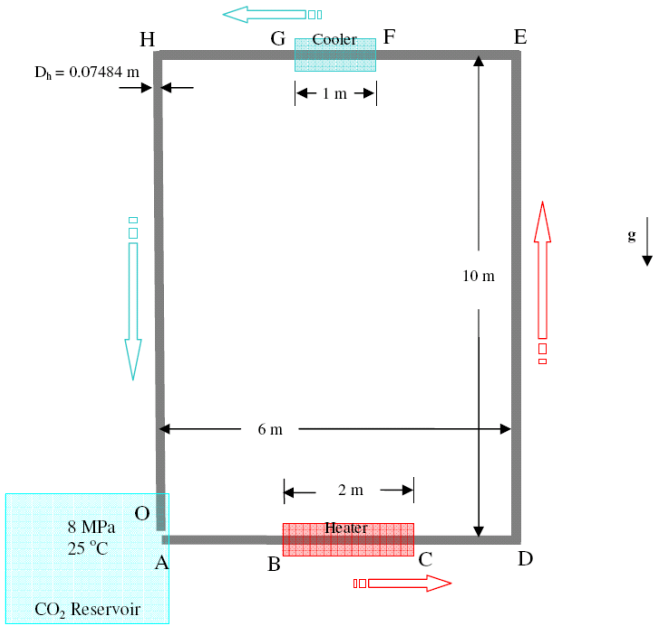

Figure 2: Schematic diagram of the flow loop

RESULTS AND DISCUSSION

Steady-state solution is determined by solving the steady state governing equations for the one-dimensional flow channel, which can be obtained by setting the time derivative of different property variables equal to zero, in the unsteady mass, momentum and energy conservation equations (see equations 1 to 3). This corresponds to $\eta = 0$ in the finite difference equations derived earlier. Steady-state behavior of the natural circulation loop with supercritical fluid is simulated at different power levels while maintaining the inlet condition constant. The results in Figure 3(a), obtained with a grid size of Δx = 0.1 m, show that the steady-state flow rate initially increases with power, reaches a maximum at about 2 MW and then decreases. While comparing steady-state results obtained using FIASCO with those obtained using the SPORTS code (shown in Figure 3(b)), it is observed that the two flow-power curves match fairly well for low values of power. However, there exists some discrepancy in the after-peak region.

Initial round of transient analyses with the FIASCO code is carried out with a spatial grid size of 0.1 m and time step size of 0.35 sec (same as in [11]). Flow is perturbed at each steady state, and the growth or decay of perturbation over time indicates whether the system at this steady state is unstable or stable, respectively. Inlet velocity evolution for three different power levels is shown in Figure 4. From the results shown in Figure 4, it is clear that the flow oscillations at 1.50 MW decay, i.e. the system is stable, and the flow oscillations at 1.53 MW grow, i.e. the system is unstable, and hence the power threshold for stability for this system is between 1.50 < P < 1.53 (MW). This is in good agreement with the results reported in [11] for the same spatial grid size and time step and shown in Figure 3(b).

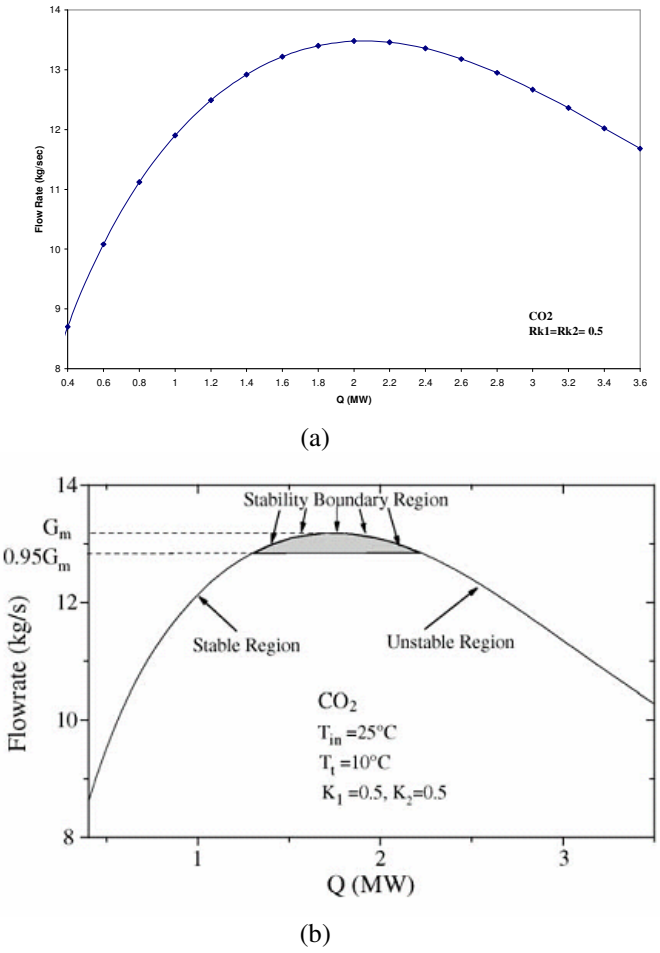

Figure 3: Steady state flow rate profile for CO_2 with 0.1 m grid size (a) FIASCO; (b) Chatoorgoon et al. (2005) [11]

In an attempt to reproduce the results reported by previous investigators, results presented in Figure 4 were obtained with Δz = 0.1 m and Δt = 0.35 sec. However, to ensure temporal and spatial grid independency of the results, grid refinement study is performed and the results, presented in the sections below, show that stability threshold does in fact change as spatial and temporal steps are refined.

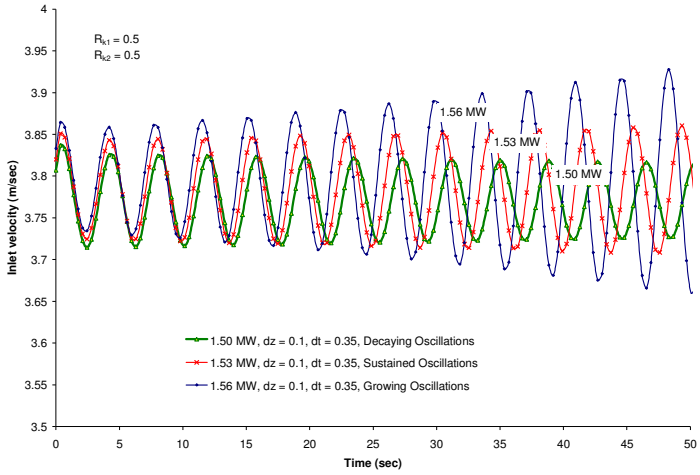

Figure 4: Inlet velocity as a function of time for three different power levels. The stability boundary is between 1.50 MW and 1.53 MW (with Δz = 0.1 m and Δt = 0.35 sec)

Effect of temporal grid refinement

For the temporal grid refinement study, 1 MW power, that is well below the stability boundary of ~1.53 MW, is chosen, and the system is predicted to be highly stable for the spatial grid size of 0.1 m and the time step size of 0.35 sec. As shown in Figure 5, further reducing the time step to half and quarter values produce sustained and growing flow oscillations, respectively. This shows the high sensitivity of the numerical approach on the time step size. It is deduced that large time step induces numerical diffusion and hence (artificial) flow stability into the system. Therefore, it is concluded that Δt = 0.35 sec is most likely too large a time step for accurate stability analysis. Further reductions of the time step yield the time-step size independent converged solution for 0.021875 (0.35/16) sec time step, as shown in Figure 6. It should be noted that though temporal grid refinement steps are not reported in [12], results presented in that reference are obtained with time step closer to 0.02 sec.

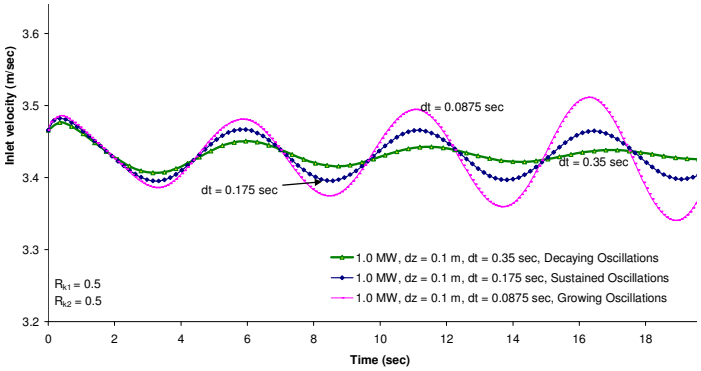

Figure 5: Effect of reducing time step on the transient solution at 1.0 MW

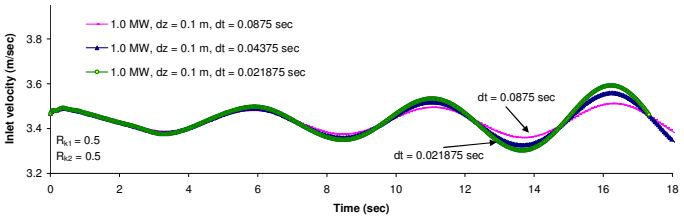

Figure 6: Further time step refinement at 1.0 MW

Effect of spatial grid refinement

To ensure the convergence of the numerical solution, a spatial grid refinement study is also performed. Effects of different grid size on the numerical solution are shown in Figures 7 and 8 for 1.0 MW and 0.7 MW power, respectively.

In Figure 7, temporal variation in inlet velocity is presented for different spatial grid sizes at 1.0 MW power. Note that the time step used for results in this figure is 0.35 sec. [Though the system is seen to be stable for this time step, as shown in Figure 7, the system is actually unstable at smaller time step values.] It can be seen that reducing the spatial grid size does not have a significant effect on system stability, as the system remains stable at finer spatial resolutions producing spatially converged results. Though a shift in oscillations is observed, but, magnitude and frequency of oscillations remain the same.

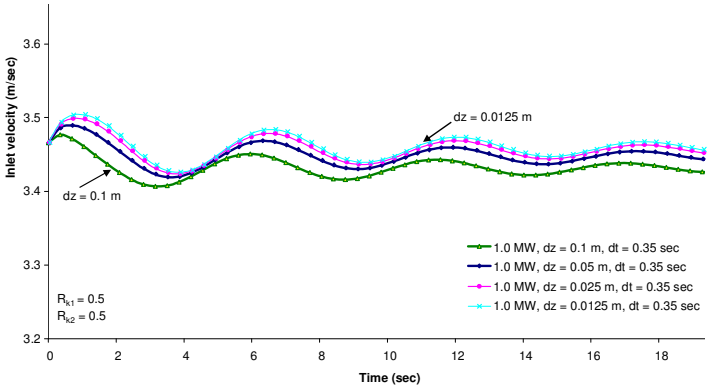

Figure 7: Effect of reducing spatial grid size on the transient solution at 1.0 MW

Furthermore, to predict the effect of spatial grid resolution on *actual* stable system, grid refinement study is performed at 0.7 MW power level and results obtained using Δt = 0.02 sec are presented in Figure 8. Once again, it is clear that a nearly stable system remains so as Δz is refined, suggesting that Δz ≃ 0.1 m is adequate for the stability analysis of this system.

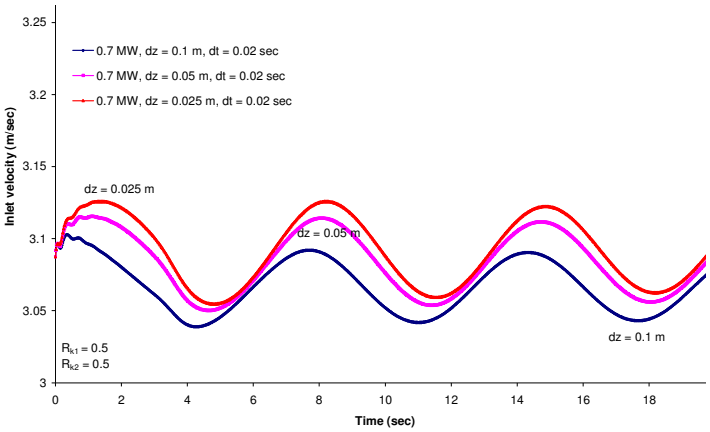

Figure 8: Effect of reducing spatial grid size on the transient solution at 0.7 MW

Effect of stringent pressure boundary tolerance

In order to accurately predict the stability boundary of the system, it is noted that pressure boundary condition at the outlet of the channel should be strictly satisfied. Otherwise, the results could be misleading. The effect of tolerance allowed in the imposition of pressure boundary condition at the exit (pb) on the numerical evaluation of system stability is shown in Figure 9. It is clear that an unstable system can be predicted to be stable if the tolerance is too large. It is concluded that a pressure boundary tolerance equal to or less than 10^{-6} MPa yields a converged solution, and should be used in the numerical simulations.

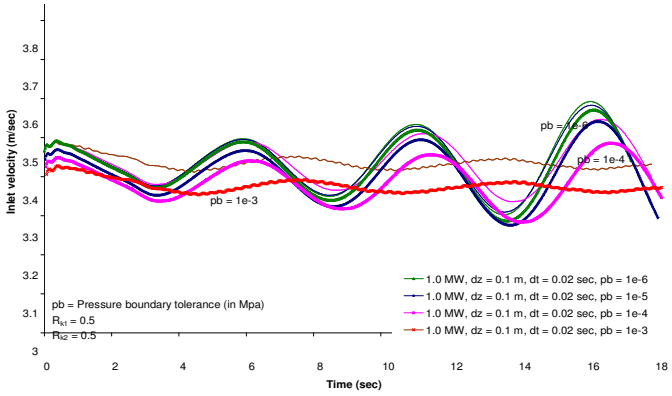

Figure 9: Effect of pressure boundary tolerance at 1.0 MW

Prediction of stability boundary

To locate the stability boundary on the steady state flow-power curve, applied power is incrementally varied, and the time-dependent set of conservation equations are numerically solved with the temporal and spatial grid size of 0.02 sec and 0.1 m respectively, until the point where sustained or growing flow oscillations are obtained. Spatial grid size was retained as 0.1 m to predict stability limit as reducing it further did not show any effect on stability, although a shift in oscillations is observed. Tolerance for exit pressure boundary condition is set at 10^{-6} MPa. Transient solutions for 0.70 MW and 0.80 MW lead to stable and unstable flow oscillations, respectively. Results are shown in Figure 10. Stability threshold is hence found to be near 0.75 MW.

It must be noted that the results obtained for stability boundary using the FIASCO code deviate substantially from the results reported in [11]) (see Figure 11). The disagreement in results is most likely due to the undesirable dissipative and dispersive effects produced from the large time steps used in reported studies, thereby leading to a larger stable region than those found using smaller time steps. This analysis further shows disagreement with the *near-peak* stability margin region as reported in [11], and shown in Figure 3(b). Results reported here are also supported by the linear stability analysis of the natural circulation loop, reported in [12], where it was also concluded that the beginning of instability is not strictly restricted to the peak region of the steady state flow-power curve. Moreover, very recently, linear stability analysis results are reported in [18] for supercritical flow in a natural-convection loop. Though, predicted stability boundaries from this approach were in close agreement to the SPORTS predictions, however, a significant difference in oscillation periods were reported. Linear solutions always predicted smaller oscillation periods than the SPORTS predictions. Therefore, it is realized that, more numerical studies for various loop configurations must be performed in order to resolve the inconsistency in different predictions and to redefine the stability regime.

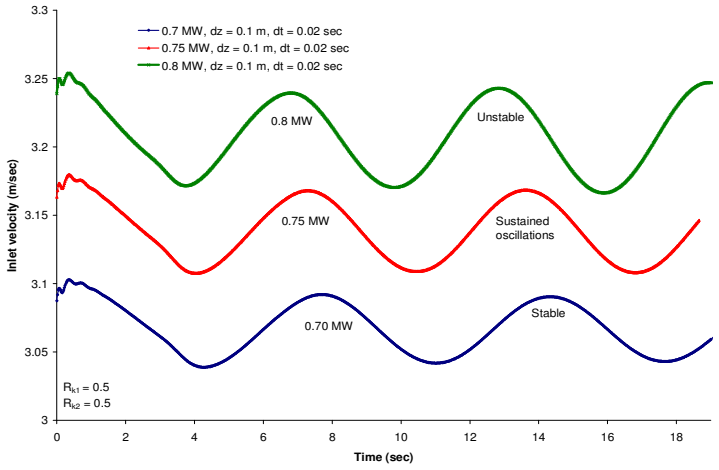

Figure 10: Transient solution for three power levels

The stability characteristics of the CO_2 natural circulation loop are predicted using the FIASCO code for different operating conditions and geometric parameters, in order to understand their influence on stability.

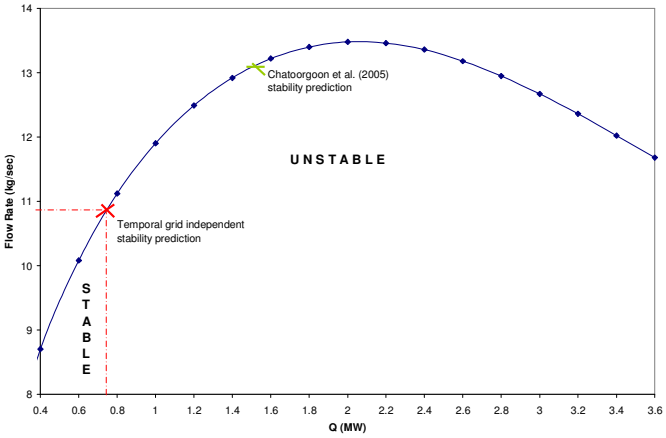

Figure 11: Comparison of stability prediction with previous investigations

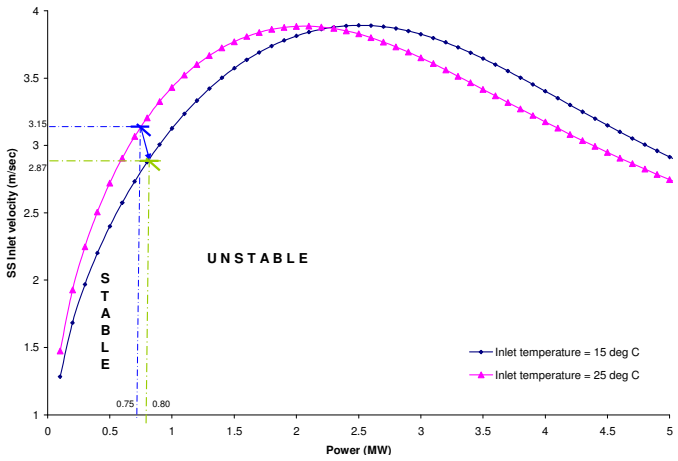

Figure 13: Effect of inlet subcooling on the stability boundary

Effect of pressure on the stability boundary

For the CO_2 natural circulation loop under supercritical conditions, an increase in system pressure (while keeping other system parameters constant) is found to have a stabilizing effect. Figure 12 shows the stability threshold on the flow-power curve for two pressure levels. Changing system pressure from 8 MPa to 10 MPa, increased the threshold power by 0.20 MW to about 0.95 MW

Effect of inlet subcooling on stability boundary

Similar to increasing system pressure, an increase in inlet degree of subcooling from 6 ^oC to 16 ^oC leads towards 0.05 MW increase in threshold power and thus stabilizes the flow system, as shown in Figure 13. Here, degree of subcooling is defined with reference to the critical temperature of CO_2 (31 ^oC). Unlike the case with pressure increase which leads to a higher flow rate at the new threshold power, an increase in degree of subcooling leads to a lower flow rate at the new stability threshold.

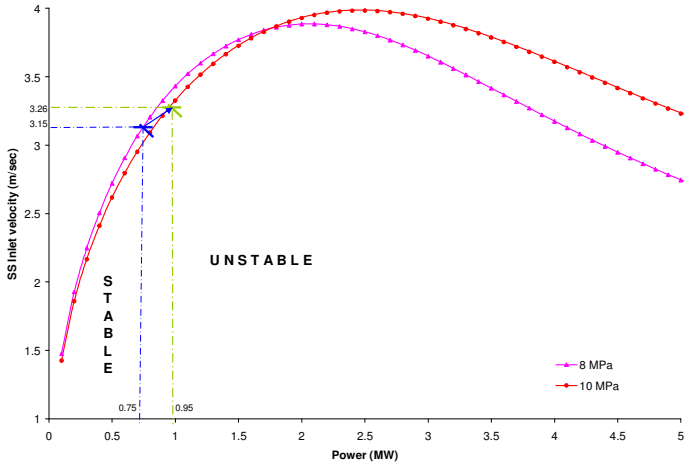

Figure 12: Effect of pressure on the stability boundary

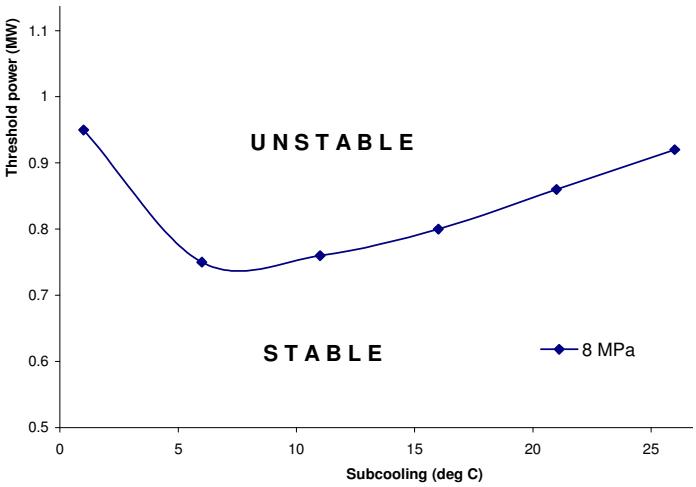

Figure 14: Effect of inlet subcooling on threshold power

Figure 14 shows the stability map plotted in the power-subcooling plane. It is observed that the effect of inlet subcooling on flow stability exhibits a minimum. For small subcoolings, increase of inlet subcooing destabilizes the flow whereas for high subcooling the effect is stabilizing. Similar behavior is also observed in various two-phase heated channels systems [17].

CONCLUSION AND FUTURE WORK

Results obtained here for the stability boundary deviate from the results reported by previous investigators, and thus contradict some of the earlier findings. The discongruity in results is possibly due to artificial dissipative and dispersive effects of large temporal grid size used in previous studies. Thus, it can be concluded from the analysis that the stability threshold power of a natural circulation loop with supercritical fluid, is not confined to the *near-peak region* of the (steady state) flow-power curve. However, results obtained for the range of parameter values used in this investigation always

predict the threshold power to be in the positive slope region of the (steady state) flow-power curve. Parametric studies for different operating conditions reveal the similarity of stability characteristics under supercritical conditions with those in two-phase flows.

To resolve the inconsistency in stability predictions, following issues are recommended for future studies:

- Due to lack of experimental studies performed with supercritical fluids in a natural circulation loop, presently there are not enough experimental data available to benchmark numerical findings. Therefore, more experimental studies should be carried out in order to support the modeling and simulation work.
- To avoid the numerical inconsistencies and uncertainties associated with time domain stability analysis, a generalized linear stability model should be developed to predict natural circulation loop behavior under supercritical operating conditions. Although similar models have been developed and reported in [12, 18], however, there still remains inconsistency in predicting stability behavior as results reported consistently deviate from the experimental findings.
- Developed model is easily extendable in time-domain to predict the onset of density-wave instability in reference design of SCWR by considering equivalent fuel channel with or without water rods.
- In order to accurately simulate the experimental stability predictions of the ANL CO2 loop [13] as well as the University of Wisconsin-Madison SCW loop [12], the assumption of fluid reservoir at the inlet and exit of flow channel should be relaxed by the application of periodic boundary conditions. It may be done by guessing all the property variables at the inlet of the flow channel, marching towards the end of the channel and match all the variables at the exit with the inlet ones for each time step. However, this approach will be computationally inefficient and highly time consuming.

REFERENCES

[1] Yamaji, A., Oka, Y., Koshizuka, S., 2005. Three-dimensional core design of high temperature supercritical-pressure light water reactor with neutronic and thermal-hydraulic coupling. Journal of nuclear science and technology 42 (1), 8-19.

[2] Generation IV International Forum (GIF), 2002. A technology roadmap for the Generation IV nuclear energy systems. GIF-002-00.

[3] Pioro, I.L., Khartabil, H.F., Duffey, R.B., 2004. Heat transfer to supercritical fluids flowing in channels ─ empirical correlations (survey). Nucl. Eng. Des. 230, 69-91.

[4] Zappoli, B., 2003. Near-critical fluid hydrodynamics. C. R. Mecanique 331, 713-726.

[5] Yang, W. S., Zavaljevski, N., 2003. Preliminary investigation of power-flow instabilities of supercritical water reactor, ANL, Technical Report.

[6] Yang, W. S., Zavaljevski, N., 2004. Effect of water rods and heat transfer correlations on SCWR stability. ANL, Technical Report.

[7] Tong, L.S., Tang, Y.S., 1997. Boiling heat transfer and two-phase flow. second edition, Taylor and Francis.

[8] Chatoorgoon, V., 2001. Stability of supercritical fluid flow in a single-channel natural-convection loop. Int. J. Heat Mass Transfer 44, 1963-1972.

[9] Chatoorgoon, V., 1986. SPORTS ─ A simple thermalhydraulic stability code. Nucl. Eng. Des. 93, 51-67.

[10] Chatoorgoon, V., Voodi, A., Fraser, D., 2005. The stability boundary for supercritical flow in natural convection loops, part I: H_2O studies. Nucl. Eng. Des. 235 (24), 2570-2580.

[11] Chatoorgoon, V., Voodi, A., Upadhye, P., 2005. The stability boundary for supercritical flow in natural convection loops, part II: CO_2 and H_2. Nucl. Eng. Des., 235 (24), 2581-2593.

[12] Jain, R., 2005. Thermal-hydraulic instabilities in natural circulation flow loops under supercritical conditions. PhD Thesis, University of Wisconsin Madison, USA.

[13] Lomperski, S., Cho, D., Jain, R., Corradini, M. L., 2004. Stability of a natural circulation loop with a fluid heated through the thermodynamic pseudocritical point. In: Proceedings of ICAPP'04, Pittsburgh, PA, USA, June 13-17, Paper 4268.

[14] Lemmon, E.W., McLinden, M.O., Huber, M.L., 2002. NIST Reference Fluid Thermodynamic and Transport Properties – REFPROP, version 7.0. US Department of Commerce, Technology Administration, National Institute of Standards and Technology.

[15] McAdams, W. H., 1954. Heat Transmission. 3d. ed., New York: McGraw-Hill.

[16] Voodi, V. A., 2004. Analytical study of non-dimensional parameters governing supercritical flow instabilities. MSc Thesis, University of Manitoba, Canada.

[17] Boure, J. A., Bergles, A. E., Tong, L. S., 1973. Review of two-phase instability. Nucl. Eng. Des. 25, 165-192.

[18] Chatoorgoon, V., Upadhye P., 2005. Analytical studies of supercritical flow instability in natural convection loops. In: Proceedings of the 11th International Topical Meeting on Nuclear Reactor Thermal-Hydraulics (NURETH-11), Avignon, France, October 2-6, Paper 165.